Structural controllability of ecological networks

Supporting Information

Fernando Cagua, Kate L. Wootton, Daniel B. Stouffer

S1 Characteristics of the empirical networks

The networks studied had species richness ranging between 19 and 87 when considering only the largest component in each network). As shown by the network asymmetry *AS* (N. Blüthgen, Menzel, Hovestadt, Fiala, & Blüthgen, 2007), the networks had a low ratio of plants to pollinators overall. Furthermore, the networks had relatively low levels of nestedness (when measured using the quantitative version of the NODF index; Almeida-Neto & Ulrich, 2011). Details for each network can be found in the Table S1.

Table S1: Properties of the analysed plant-pollinator communities. Here show the number of species (n_s), the number of plants (n_p), the number of pollinators (n_a), the network connectance (c), the network asymmetry (AS), and the network nestedness (NODF index). All properties correspond to the network's largest component. British networks were assembled by Lopezaraiza-Mikel et al. (2007), Spanish were networks assembled by Bartomeus et al. (2008).

site	invader	n_s	n_p	n_a	c	AS	NODF	location
1	—	35	9	26	0.17	-0.49	8.68	Cap de Creus, Spain
1	*Carpobrotus affine*	57	10	47	0.17	-0.65	13.27	Cap de Creus, Spain
2	—	40	10	30	0.16	-0.50	11.66	Cap de Creus, Spain
2	*Carpobrotus affine*	38	11	27	0.21	-0.42	15.04	Cap de Creus, Spain
3	—	31	7	24	0.19	-0.55	12.91	Cap de Creus, Spain
3	*Opuntia stricta*	33	8	25	0.18	-0.52	9.96	Cap de Creus, Spain
4	—	35	10	25	0.17	-0.43	12.43	Cap de Creus, Spain
4	*Carpobrotus affine*	57	14	43	0.14	-0.51	13.70	Cap de Creus, Spain
5	—	35	8	27	0.19	-0.54	11.91	Cap de Creus, Spain
5	*Opuntia stricta*	32	8	24	0.19	-0.50	10.96	Cap de Creus, Spain
6	—	30	9	21	0.17	-0.40	6.91	Cap de Creus, Spain
6	*Opuntia stricta*	37	9	28	0.17	-0.51	12.45	Cap de Creus, Spain
7	—	37	6	31	0.19	-0.68	18.33	Bristol, United Kingdom
7	*Impatients grandulifera*	57	8	49	0.20	-0.72	14.36	Bristol, United Kingdom
8	—	48	5	43	0.21	-0.79	5.87	Bristol, United Kingdom
8	*Impatients grandulifera*	87	15	72	0.11	-0.66	8.12	Bristol, United Kingdom
9	—	55	12	43	0.13	-0.56	13.01	Bristol, United Kingdom
9	*Impatients grandulifera*	86	11	75	0.13	-0.74	13.40	Bristol, United Kingdom
10	—	19	3	16	0.38	-0.68	9.99	Bristol, United Kingdom
10	*Impatients grandulifera*	54	6	48	0.21	-0.78	7.56	Bristol, United Kingdom

S2 Structural controllability

Structural controllability avoids the limitation of not knowing the exact values of the matrices A and B. Using structural controllability can be boiled down to two conditions: a system is controllable if there are no inaccessible nodes or dilations. A node is inaccessible if there are no directed paths between it and the input nodes. "Dilations are subgraphs in which a small subset of nodes attempts to rule a larger subset of nodes. In other words, there are more 'subordinates' than 'superiors' " (Liu & Barabási, 2016).

The goal of structural controllability is to use the information contained in **A** to generate a supportable estimate of **B**. This focus allows us to gain insight of the inherent controllability of a network, and the roles of the species that compose it, without being overly dependent on the particular choices of how the system dynamics are modelled or characterised. The trade-off of this approach is that, because of the assumption of linearity, structural controllability alone does not allow us to fully design the time-varying control signal $u(t)$ that can drive the system from one particular equilibrium to another. Nevertheless, the lessons gained when assuming linearity—at both the network and the species level—are a prerequisite for eventually understanding nonlinear control (Liu & Barabási, 2016; Liu, Slotine, & Barabási, 2011).

S3 Maximum matching

S3.1 Finding a single maximum matching

Our approach to finding the minimum number of driver nodes relies on finding maximum matchings. We start with a directed network in which the direction of the link represents the direction of control (Figure S1 left panel). We then construct an alternative representation of the directed network in which each node of the directed network is represented by two nodes that indicate their outgoing and incoming links respectively (Figure S1 centre panel). Finding a maximum matching in this alternative representation is equivalent to finding the largest possible set of edges in which one node on the left-hand side is connected to at most one node on the right-hand side. To find the maximum matching we use the push-relabel algorithm implemented in `max_bipartite_matching` in the R package igraph 1.0.1 (Csardi & Nepusz, 2006). Once we have the matching (shown in the Figure S1 center panel) it is then easy to identify the roles of each node in this representation: nodes on the top-level that are connected to a matched link (dark purple) are superior while those connected to a matched link on the bottom-level are matched. This information can then be mapped back to the original representation to identify the control paths and the driver nodes in the network (Figure S1 right panel).

To further illustrate our methodology here, we also show the approach for the smallest of our empirical networks, the uninvaded network at site 10 (Table S1; Figure S2). This network is composed of 19 species of which three are non-invasive plants and the other 16 are pollinators. The one-to-one relationship between matched and superior nodes implies that in order to achieve full network controllability, most pollinators would be unmatched, and hence are classified as driver nodes that require external intervention. At the same time, both plants in the community, *Heracleum sphondylum* and *Rubus fructicosus*, and one of the pollinators, *Orthotylus/Lygocorus*, tend to be classified as superior nodes.

S3.2 Finding all possible maximum matchings

The algorithm implemented in `max_bipartite_matching`, however, is only able to find **one** of possibly many maximum matchings in a network. Though one maximum matching is enough to calculate n_D and hence to provide an indication of the manageability of a community, it is not sufficient to estimate the role of individual species. To do that, we need to calculate all possible maximum matchings (or, equivalently, all maximal cardinality matchings in weighted networks like ours). To do this, we again start from the alternative bipartite representation in Figure S1b and assign an identity to each of the links in the network. We will call this bipartite representation P. We then construct the line graph of the alternative bipartite representation $L(P)$ (Figure S3). Each node in $L(P)$ represents a link in P and these are connected to each other if and only if they share a common node in P. We then calculate H, the

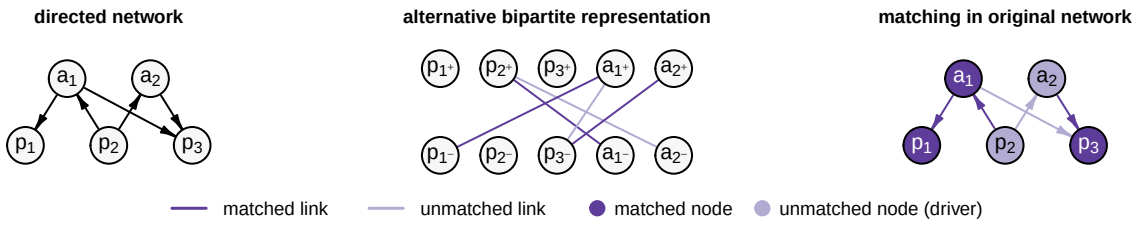

Figure S1: Finding a maximum matching in a complex network. (left) Directed network that indicate the direction of control between species. (center) Alternative bipartite representations of the directed networks. (right) The matchings in the bipartite representation mapped back to the original network.

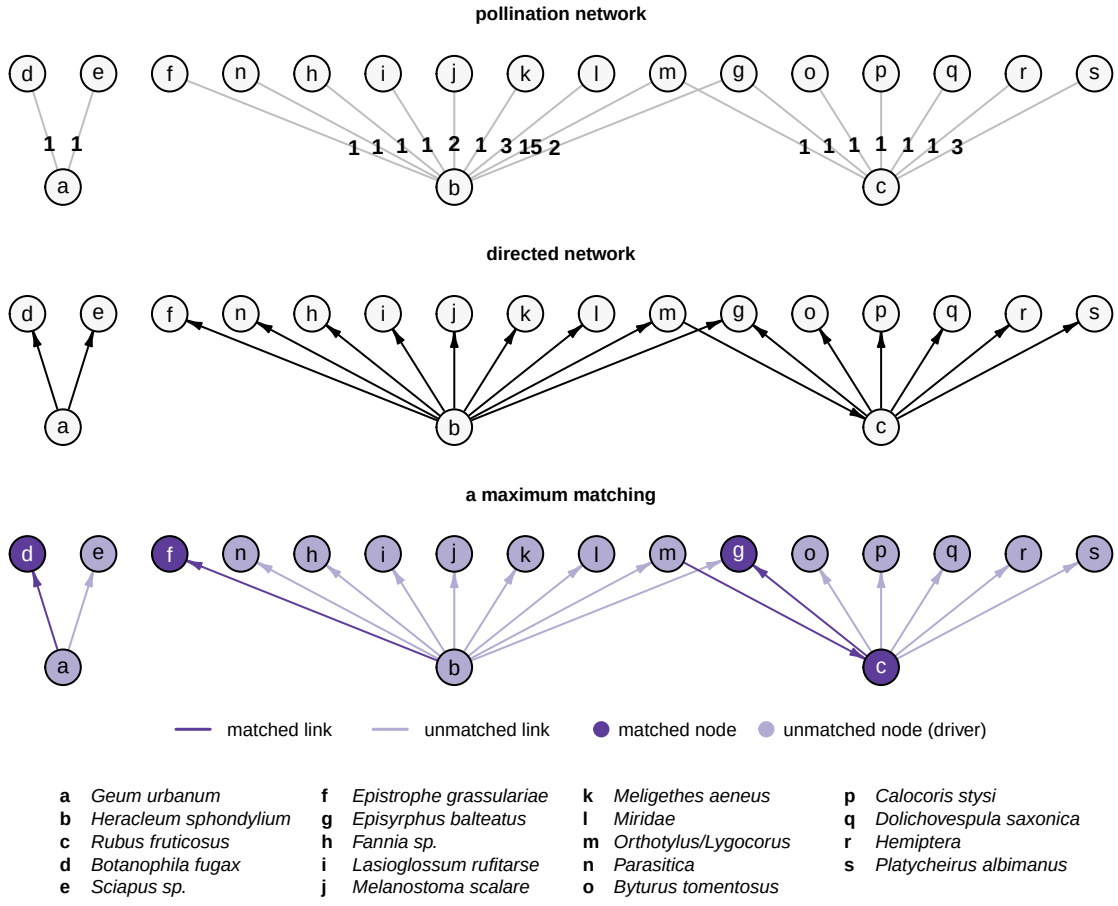

Figure S2: Illustration of the procedure with an empirical community. The visitation network (top), the number of visits between species pairs are shown on each link. The directed network in which the direction of control is determined based on the mutual dependences (middle). One of the possible maximum matchings of this network (bottom).

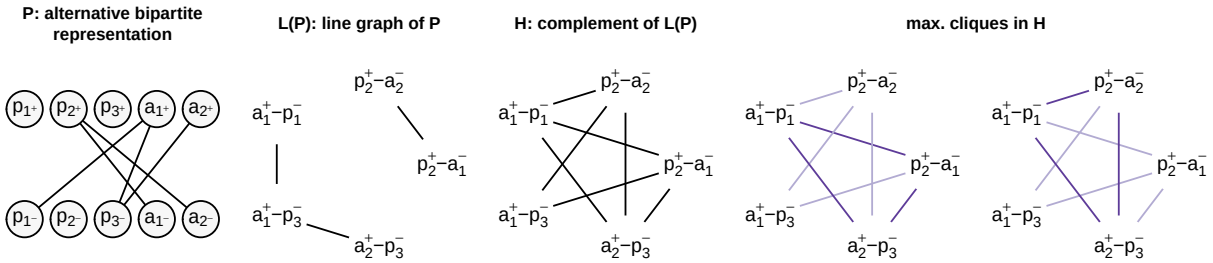

Figure S3: Finding all possible maximum matchings. From left to right: alternative bipartite representation of the directed network. Line graph of the network. The complement of the network. The two maximal cliques are shown in dark purple.

complement graph of $L(P)$ and identify all of its maximal cliques (Figure S3). Here some extra definitions are necessary. First, H is a graph with the same nodes as $L(P)$ but that has a link between two nodes if and only if there is not a link in $L(P)$. Second, a clique is a subset of nodes such that all pairs of them are linked. Lastly, a maximal clique is a clique such that there are no cliques composed of more nodes (Gutin, 2013). In this example, there are two maximal cliques: the one formed by 1, 3 and 5, and the one formed by 2, 3 and 5. The final step is then to map these cliques onto the original network to obtain all possible maximal cardinality matchings as shown in Figure 2 in the main text.

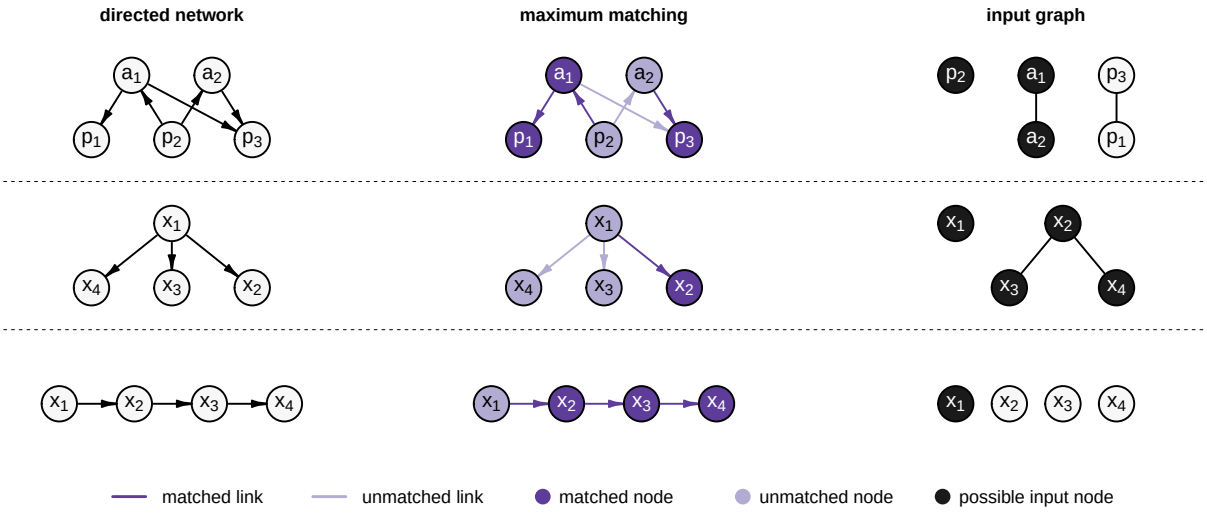

Figure S4: Input graph. Two nodes x_i and x_j are said to be control adjacent if there is a node x_k connecting x_i and x_j with an unmatched link $x_k - x_i$ and a matched link $x_k - x_j$. For example, in the top panel, a_1 is control adjacent to a_2 (via p_2), p_1 is control adjacent to p_3 (via a_1) and p_2 has no control adjacent nodes. As a_1 and p_2 belong to the minimum driver node set under the control configuration found with the maximum matching shown, then every node in the same component as these two nodes is also a possible driver node. By combining the nodes from the components with minimum driver node sets is possible to enumerate the different control configurations. For example the network in the top panel has two possible minimum driver node sets $[p_2, a_1]$ and $[p_2, a_2]$ (Figure 2). The network in the middle panel has three minimum driver node sets $[x_1, x_2]$, $[x_1, x_3]$, and $[x_1, x_4]$. Finally the network in the bottom pannel has only one $[x_1]$.

S3.3 Control adjacency and the input graph

The algorithm proposed by Zhang, Lv, & Pu (2016) enable us to find all minimum driver node sets without calculating all possible maximum matchings. The algorithm is based on the construction of the input graph of the directed network. Components in the input graph reveal the correlations between nodes from a structural control perspective (Figure S4). The input graph is constructed based on the *control adjacency* of nodes in a maximum matching. Two nodes x_i and x_j are said to be control adjacent if there is a node x_k connecting x_i and x_j with an unmatched link $x_k - x_i$ and a matched link $x_k - x_j$. For example a_1 is control adjacent to a_2 in the top panel of Figure S4. If a node x_i is part of a minimum driver node set then every node in the same component of x_i in the input graph is a possible driver node.

In order to calculate a node's control capacity ϕ, we harness the fact that nodes can be classified into three groups according to their role in the input graph. First, if x_i belongs to the minimum driver node set and has no adjacent nodes, then it cannot be replaced and will be part of every possible control configuration. Second, if x_i does not belong to the minimum driver node set and is not adjacent to any possible input node, then it does not part of the minimum driver node set under any control configuration. Finally, if a node x_i belongs to the minimum driver node set and is adjacent to another node x_j in the input graph, then x_j must belong to another minimum driver node to which x_i does not belong, in other words, x_i and x_j are substitutable.

The frist and the second group have a control capacity of $\phi = 1$ and $\phi = 0$ respectively. Meanwhile, the third group has intermediate values of control capacity which can be calculated by computing the number of possible substitutions of a node by its control adjacent nodes. As a rule of thumb, the largest the number of possible substitutions an input node has, the smaller its control capacity.

For larger networks, calculating the control capacities using the input graph is several orders of magnitude faster than computing all possible maximum matchings. While the computation time of the input graph grows linearly with network size, the computation of all maximum matchings grows polynomially. However, the control capacities obtained using the input graph are not identical to those obtained by computing all possible maximum matchings. The reason for this discrepancy is that two maximum matchings might result in the same minimum driver node set. Nevertheless, the results obtained using both approaches are extremely similar. We compared the control capacity obtained by calculating all maximum matchings and that obtained using the input graph in 13 of our networks (those for which we were able to calculate all maximum matchings within a reasonable time). The spearman correlation was very high in all cases, ranging between 0.89 and 1 (median 0.98).

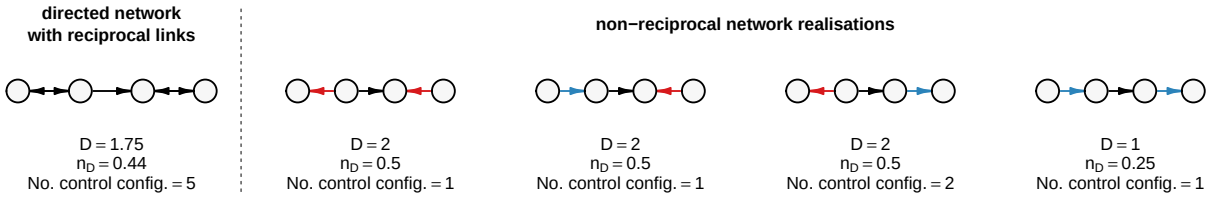

Figure S5: In order to calculate the controllability metrics for a network with reciprocal links (left), we first decompose the network into several versions that contain no reciprocal links (right). As each of these networks represents a different equiprobable scenario, the controllability metrics for the network with reciprocal links are the unweighted mean of these metrics across the non-reciprocal networks.

S3.4 Networks with reciprocal links

Our procedures to find minimum driver node sets are only adequate when there are no reciprocal (bidirectional) links in the network. The proportion of reciprocal links in relatively low. In fact, the proportion of species pairs that are reciprocally connected in our empirical networks is just 2.97%. However, reciprocal links are not a rare occurrence as 16 out of 20 empirical networks had at least one. To calculate our controllability metrics at both the network (the relative size of the minimum driver node set, n_D) and species level (control capacity, ϕ, and the likelihood of being a superior node, σ) we first need to generate all possible versions of the of the network that include only non-reciprocal links (Figure S5).

All of these non-reciprocal networks are as likely to be one that best represents the superior/matched relationships in the network. As such, we average the three metrics (n_D, ϕ, and σ) across all the networks without reciprocal links without weighting by the number of possible control configurations.

S4 Structural stability

We follow R. P. Rohr, Saavedra, & Bascompte (2014) and S. Saavedra, Rohr, Olesen, & Bascompte (2016) to calculate the structural stability of the empirical networks. We first calculate the stability condition $\hat{\gamma}$ using all species in the network. To simplify the calculations we assumed that there is no mutualistic trade-off, and a mean field interspecific competition of $\rho = 0.005$ (S. Saavedra et al., 2016). To calculate the contribution to stable coexistence of a given species, we removed the focal species from the network and then calculated the corresponding structural feasibility Ω for a level of mutualism equal to the stability condition found previously. The choice of the parameters, specifically the interspecific competition ρ had only a small impact on the relative contribution of species to stable coexistence (Figure S6a).

In addition, the interspecific competition had a minor impact on our result that indicates that critical species (those with $\phi = 1$) have a larger than average contribution to stable coexistence (Figure S6b).

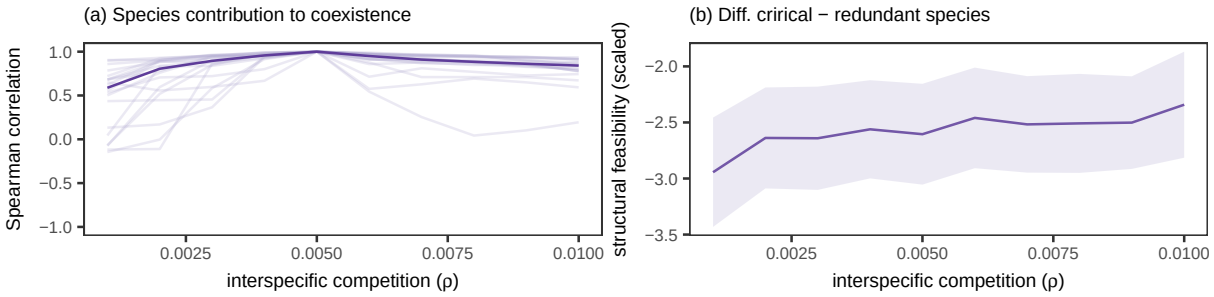

Figure S6: A sensitivity analysis of the impact of interspecific competition parameter ρ on structural stability reveals that the choice of parameters has a negligible impact on the results. (a) Spearman correlation coefficient of the contribution to stable coexistence of species. Lighter lines indicate the correlation coeficient for each of the twenty empirical networks. The dark line indicates the median value. (b) Difference between the conribution to stable coexistence of critical and redundant species for different values of the iterspecific competition parameters ρ.

S5 Visitation as a proxy for species dependence

Visitation frequency has been shown to be an appropriate surrogate for inter-specific effects in pollination networks (Bascompte, Jordano, & Olesen, 2006; Vázquez, Morris, & Jordano, 2005). Nevertheless, visitation is not equivalent to pollen deposition and might be insufficient to reflect the dependences of plants on animals and vice versa (Alarcón, 2010; King, Ballantyne, & Willmer, 2013). We, therefore, investigated the effect of calculating the dependences using visitation or pollination effectiveness and importance—two metrics more proximate to plant reproductive success. We did this by comparing *(i)* the size of the minimum driver node set n_D of the community, *(ii)* the species' control capacity and, *(iii)* the species' probability of being a superior node. To do this, we used data collected by G. Ballantyne, Baldock, & Willmer (2015) from a low diversity pollination community at a dry lowland heathland in Dorset, UK (50° 43.7'N 2° 07.2'W). First, deposition networks were quantified using the mean single visit deposition—the number of conspecific pollen grains effectively deposited on a virgin stigma during a single visit by a particular animal (G. Ballantyne et al., 2015; King et al., 2013; Ne'eman, Jürgens, Newstrom-Lloyd, Potts, & Dafni, 2009). Second, visitation networks were constructed by counting the visits to flowers during Single Visit Depositions. Finally, pollinator importance networks were constructed as the product of pollinator efficiency and visit frequency.

At a network scale the driver-node density n_D was consistent among the three weighting schemes (0.67 for deposition, 0.67 for the visitation, and 0.62 for the pollinator-importance network, respectively). The choice of weighting can also have an impact on at the species level. Therefore we calculated ϕ and σ and calculated it's correlation among all three weighting schemes. Although visitation and efficiency (pollen deposition) produce moderately different results, we found a very strong agreement between the order produced by visitation and importance which is arguably a more accurate metric of interspecific effects (Table **??**).

Table S2: Spearman correlation coefficient matrix between the control capacity and the probability obtained by weighting links by the visitation, pollinator efficiency and pollinator importance.

	efficiency	importance	visitation
control capacity			
efficiency	1.00	0.37	0.38
importance	0.37	1.00	0.86
visitation	0.38	0.86	1.00
superior probability			
efficiency	1.00	0.69	0.57
importance	0.69	1.00	0.90
visitation	0.57	0.90	1.00

Altogether, the evidence supports the idea that visitation is a suitable metric to estimate the mutual dependence of species pairs. First, it is directly related to pollinator foraging. Second, it produces results within our controllability framework that are consistent with plant reproductive success (as estimated by

the importance metric).

S6 Sensitivity to sampling

Our approach is fundamentally based on the network structure. Often, the majority of the interactions that make up this structure are weak; in our networks, this means that most interactions are formed by a small number of observed pollination visits, and therefore those weak interactions are less conspicuous in the field than strong ones. To strengthen the case of our approach, we, therefore, evaluated the robustness of our results to simulated sampling limitations.

To do so we removed a portion of the visits, for each network, and calculated how three control metrics of the subsampled network compare to those of the full network. Specifically, we calculated the difference between the relative size of the minimum driver node set n_D of the subsampled and the full network, the Spearman correlation between the control capacities ϕ and the probability of being a superior node σ that were obtained for the empirical network and subsamples of it. Finally, we also compared the control capacity of critical species ($\phi = 1$) across the different subsamples. We removed up to 20% of the interactions in 1% increments. We repeated the procedure for each network to obtain a total sample size of $n = 400$.

Overall, the results of the sensitivity analysis indicate that our approach is likely to still be useful in the absence of complete sampling. Specifically, as the proportion of sampled interaction decreased, the variability of n_D increased but was overall similar to that obtained when using all available interactions (Figure S7). Similarly, the correlation between ϕ and σ of empirical and subsampled networks was high even for extreme levels of undersampling (Figure S8). Importantly, critical species in the empirical networks were also critical species in the subsampled networks in a large majority of cases (Figure S9).

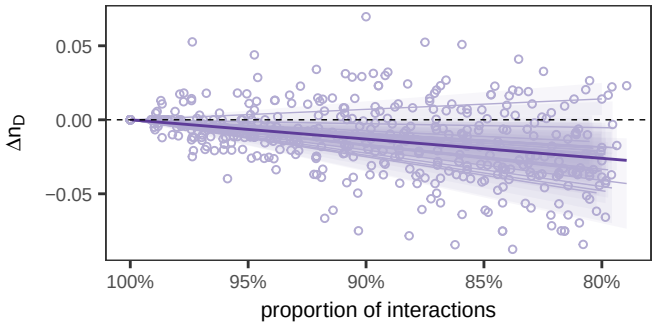

Figure S7: Difference between the size of the minimum driver node set of the empirical network and the subsampled network. Lighter lines indicate the changes for each networks and the darker line indicates the overall trend.

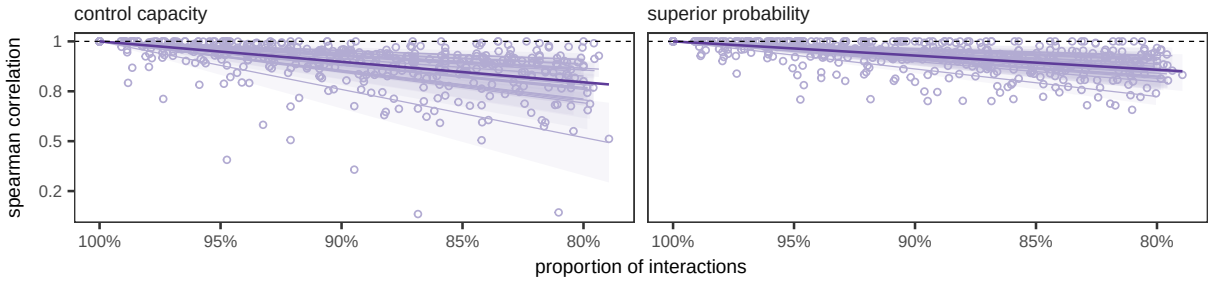

Figure S8: Spearman correlation between the control capacity and the probability of being a superior nodes of the empirical networks and subsampled networks. Lighter lines indicate the changes for each networks and the darker line indicates the overall trend.

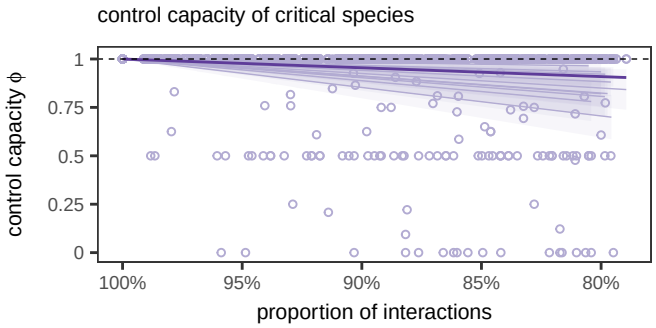

Figure S9: Control capacity of critical species (those with $\phi = 1$ in the empirical network) in subsampled networks. Lighter lines indicate the changes for each networks and the darker line indicates the overall trend.

Table S3: Model selection table based on the Akaike Information Criterion for small samples for candidate models of size of the minimum driver node set (n_D) in the empirical networks. There was no evidence for any of the evaluated predictors: the invasion status (inv), the network connectance (c), the network nestedness (NODF) the number of species (n_S) the network asymmetry (AS_s) or the interaction strength asymmetry (AS_s). Only candidate models with $\Delta AIC < 8$ are shown.

model	$AICc$	$\Delta AICc$	Cum. Weight
$n_D \sim 1$	14.12	0.00	0.20
$n_D \sim inv$	16.60	2.49	0.26
$n_D \sim C$	16.61	2.49	0.32
$n_D \sim NODF$	16.61	2.49	0.38
$n_D \sim n_s$	16.64	2.52	0.44
$n_D \sim AS_s$	16.73	2.61	0.49
$n_D \sim study$	16.73	2.61	0.55
$n_D \sim AS_n$	16.80	2.68	0.60
$n_D \sim C + inv$	19.41	5.29	0.61
$n_D \sim NODF + inv$	19.41	5.29	0.63
$n_D \sim C + NODF$	19.41	5.29	0.64
$n_D \sim n_s + inv$	19.44	5.32	0.66
$n_D \sim n_s + NODF$	19.44	5.32	0.67
$n_D \sim n_s + C$	19.48	5.36	0.69
$n_D \sim C + study$	19.53	5.41	0.70
$n_D \sim n_s + study$	19.53	5.41	0.71
$n_D \sim AS_s + NODF$	19.53	5.41	0.73
$n_D \sim inv + study$	19.53	5.41	0.74
$n_D \sim C + AS_s$	19.53	5.41	0.75
$n_D \sim NODF + study$	19.53	5.41	0.77
$n_D \sim AS_s + inv$	19.53	5.42	0.78
$n_D \sim AS_s + study$	19.55	5.44	0.79
$n_D \sim n_s + AS_s$	19.56	5.44	0.81
$n_D \sim AS_n + study$	19.59	5.47	0.82
$n_D \sim n_s + AS_n$	19.59	5.47	0.83
$n_D \sim AS_n + inv$	19.59	5.47	0.85
$n_D \sim C + AS_n$	19.59	5.47	0.86
$n_D \sim AS_n + NODF$	19.59	5.47	0.87
$n_D \sim AS_n + AS_s$	19.59	5.47	0.89

Table S4: Selection table of the random effects in the generalised mixed effect models of control capacity ϕ and the probability of being a superior node σ. Only models with a weight larger than 0.01 are shown. We modelled the probability of being a superior node without random effects as the random intercept over site had zero variance.

random effects	AICc	delta	weight
control capacity models			
asymmetry | guild	487.56	0.00	0.68
asymmetry | guild + 1 | site	489.60	2.04	0.25
visitation strength | guild + asymmetry | guild	493.71	6.15	0.03
contribution to nestedness | guild + asymmetry | guild	493.84	6.28	0.03
visitation strength | guild + asymmetry | guild + 1 | site	495.96	8.40	0.01
superior probability models			
1 | site	155.84	0.00	0.64
asymmetry | guild	159.91	4.07	0.08
contribution to nestedness | guild	159.91	4.07	0.08
visitation strength | guild	159.91	4.07	0.08
contribution to nestedness | guild + 1 | site	161.95	6.11	0.03
asymmetry | guild + 1 | site	161.95	6.11	0.03
visitation strength | guild + 1 | site	161.96	6.12	0.03

Table S5: Summary table of the control capacity model with the smallest AICc.

effect type	term	estimate	std. error	z value	p value
control capacity models					
fixed	(Intercept)	0.68	0.29	2.37	0.02
fixed	visitation strength	1.55	0.71	2.19	0.03
fixed	contribution to nestedness	1.05	0.17	6.03	0.00
fixed	degree	-0.69	0.46	-1.50	0.13
guild	std. dev. (guild)	1.64	—	—	—
guild	std. dev. (asymmetry | guild)	0.99	—	—	—
guild	cor. (asymmetry | guild)	-1.00	—	—	—
superior probability models					
fixed	(Intercept)	-5.42	0.67	-8.12	0.00
fixed	visitation strength	3.76	0.59	6.36	0.00
fixed	contribution to nestedness	0.38	0.20	1.90	0.06
fixed	asymmetry	7.36	0.88	8.40	0.00

Table S6: Variable importance for each set of models. The importance is the sum of the weights of all models in which the variable was included.

term	importance
control capacity models	
contribution to nestedness	1.00
visitation strength	0.91
degree	0.50
asymmetry	0.27
superior probability models	
asymmetry	1.00
visitation strength	1.00
contribution to nestedness	0.92
degree	0.30

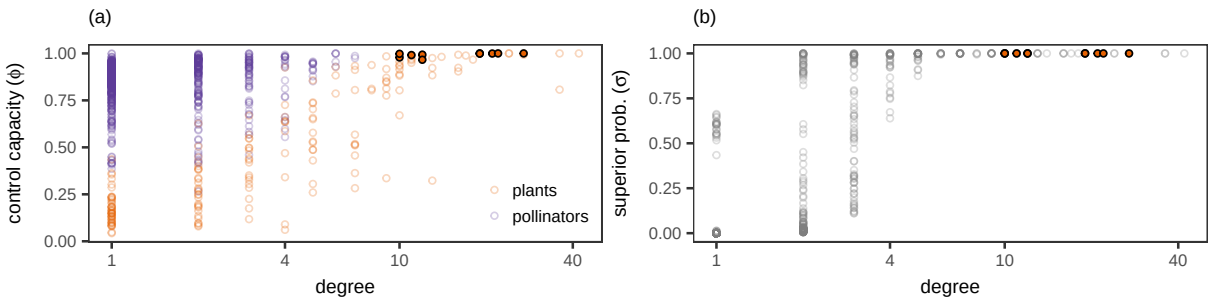

Figure S10: Relationship between degree and (a) the control capacity and (b) the probability of being a superior node. The plots show the values predicted by most parsimonious model for each response variable. The invasive species are depicted with solid orange circles.

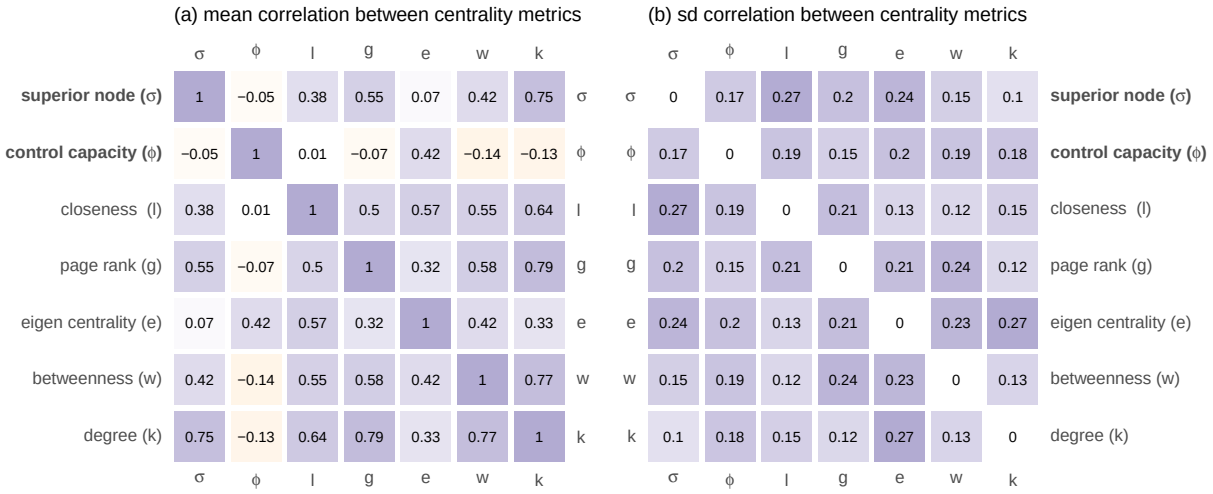

Figure S11: Mean Spearman correlation coefficients between control metrics (control capcity ϕ and the likelyhood of being a superior node σ) and centrality metrics commonly used to estimate a species' 'keystoness' (closeness centrality l , betwenness w, eigen centrality e, page rank g and degre k) in each of the networks. Purple and orange tiles indicate a positive correlation or negative correlation respectively.

References

Alarcón, R. (2010). Congruence between visitation and pollen-transport networks in a California plant-Pollinator community. *Oikos*, *119*(1), 35–44. doi:10.1111/j.1600-0706.2009.17694.x

Almeida-Neto, M., & Ulrich, W. (2011). A straightforward computational approach for measuring nestedness using quantitative matrices. *Environmental Modelling & Software*, *26*(2), 173–178. doi:10.1016/j.envsoft.2010.08.003

Ballantyne, G., Baldock, K. C. R., & Willmer, P. G. (2015). Constructing more informative plantPollinator networks: Visitation and pollen deposition networks in a heathland plant community. *Proceedings of the Royal Society B: Biological Sciences*, *282*(1814), 20151130. doi:10.1098/rspb.2015.1130

Bascompte, J., Jordano, P., & Olesen, J. M. (2006). Asymmetric Coevolutionary Networks Facilitate Biodiversity Maintenance. *Science*, *312*(5772), 431–433. doi:10.1126/science.1123412

Blüthgen, N., Menzel, F., Hovestadt, T., Fiala, B., & Blüthgen, N. (2007). Specialization, Constraints, and Conflicting Interests in Mutualistic Networks. *Current Biology*, *17*(4), 341–346. doi:10.1016/j.cub.2006.12.039

Csardi, G., & Nepusz, T. (2006). The igraph software package for complex network research. *InterJournal, Complex Systems*, *1695*(5), 1–9.

Gutin, G. (2013). Independence and Cliques. In P. Zhang (Ed.), *Handbook of Graph Theory* (Second Edi, pp. 475–489). Chapman and Hall/CRC. doi:10.1201/b16132-31

King, C., Ballantyne, G., & Willmer, P. G. (2013). Why flower visitation is a poor proxy for pollination: Measuring single-visit pollen deposition, with implications for pollination networks and conservation. *Methods in Ecology and Evolution*, *4*(9), 811–818. doi:10.1111/2041-210X.12074

Liu, Y.-Y., & Barabási, A.-L. (2016). Control principles of complex systems. *Reviews of Modern Physics*, *88*(3). doi:10.1103/RevModPhys.88.035006

Liu, Y.-Y., Slotine, J.-J., & Barabási, A.-L. (2011). Controllability of complex networks. *Nature*, *473*(7346), 167–173. doi:10.1038/nature10011

Ne'eman, G., Jürgens, A., Newstrom-Lloyd, L., Potts, S. G., & Dafni, A. (2009). A framework for comparing pollinator performance: Effectiveness and efficiency. *Biological Reviews*, no–no. doi:10.1111/j.1469-185X.2009.00108.x

Rohr, R. P., Saavedra, S., & Bascompte, J. (2014). On the structural stability of mutualistic systems. *Science*, *345*(6195), 1253497–1253497. doi:10.1126/science.1253497

Saavedra, S., Rohr, R. P., Olesen, J. M., & Bascompte, J. (2016). Nested species interactions

promote feasibility over stability during the assembly of a pollinator community. *Ecology and Evolution*, *6*(4), 997–1007. doi:10.1002/ece3.1930

Vázquez, D. P., Morris, W. F., & Jordano, P. (2005). Interaction frequency as a surrogate for the total effect of animal mutualists on plants: Total effect of animal mutualists on plants. *Ecology Letters*, *8*(10), 1088–1094. doi:10.1111/j.1461-0248.2005.00810.x

Zhang, X., Lv, T., & Pu, Y. (2016). Input graph: The hidden geometry in controlling complex networks. *Scientific Reports*, *6*(1). doi:10.1038/srep38209